Electronic Supplementary Material (ESI)

Bimetallic MOFs@Graphene Oxide Composites as Efficient Bifunctional Oxygen Electrocatalysts in Rechargeable Zn-Air Batteries

Yao Xiao[a,b], Beibei Guo[b], Jing Zhang[c], Chun Hu[b], Ruguang Ma[b], Deyi Wang[a,c*], Jiacheng Wang[b**]

[a] School of Science, Xihua University, Chengdu, 610039, China

[b] State Key Laboratory of High Performance Ceramics and Superfine Microstructure, Shanghai Institute of Ceramics, Chinese Academy of Sciences, Shanghai 200050, China.

[c] IMDEA Materials Institute, C/Eric Kandel, 2, Getafe, Madrid, 28906, Spain

Emails: jiacheng.wang@mail.sic.ac.cn; deyi.wang@imdea.org

Experimental Section

Chemicals

Cobalt nitrate hexahydrate ($Co(NO_3)_2 \cdot 6H_2O$), zinc nitrate hexahydrate ($Zn(NO_3)_2 \cdot 6H_2O$) and 2-methylimidazole were purchased from Sinopharm Chemical Reagent Co. Ltd. Methanol (CH_3OH) was purchased Shanghai Lingfeng Chemical Reagent Co. Ltd. Nafion solution (5 wt%) was purchased from Aldrich. The commercial Pt/C catalyst (20 wt%) was obtained from Johnson Matthey (UK). All solvents and chemicals were utilized as received without any further purification.

Preparation of MOF@GO nano-hybrid

GO was prepared by a Hummers' method. [1] ZnCo-ZIF@GO nano-hybrid was prepared typically as following. Briefly, 0.864 g $Zn(NO_3)_2 \cdot 6H_2O$ and 0.576 g $Co(NO_3)_2 \cdot 6H_2O$ were dissolved in 100 mL methanol (mole ratio Zn/Co=6/4). Then, 120 mg GO water solution was added into mixed metal ion solution with sonication, followed by stirring for 30 mins. Meanwhile, 2.16 g 2-MIM was dissolved in 100 mL methanol separately. Afterwards, two solutions were mixed rapidly with vigorously stirring for 2 h at 25 ^oC. The generated purple precipitates were collected and cleaned by centrifuge at 10000 rpm. The residue precursors were removed by repeating this procedure. The sample was dried in the vacuum oven at 80 ^oC overnight. [2] ZnCo-ZIF was also prepared by the same procedure without adding GO.

Characterizations

Field emission scanning electron microscopy (FESEM) was performed on FEI Magellan 400, and Transmission electron microscopy (TEM) images were collected on a JEM-2100F. Power X-ray diffraction (XRD) was obtained using a D8 ADVANCE instrument with Cu Ka1 radiation (40 kV, 60 mA). Raman spectroscopy was measured on a DXR Raman Microscope (Thermal Scientic Co., USA) with 532 nm excitation length. X-ray photoelectron spectroscopy (XPS) were recorded using an ESCALAB 250 X-ray photoelectron spectrometer using Al Kα (hv=1486.6 eV) radiation. N_2 adsorption-desorption isotherms were measured at -196 ^oC with an ASAP 2010 Surface Area and Pore Size Analyzer System (Micromeritics, Norcross, GA). The special surface area was calculated using the multipoint Brunauer–Emmett–Teller (BET). The

pore size distribution curves, pore volume and pore diameter were carried out by the adsorption branch of the isotherms using the Density- Functional- Theory (DFT).

Electrocatalytic activity evaluation

All electrochemical measurements were conducted in a three-electrode configuration using a CHI760E electrochemical workstation at room temperature (25 ^{o}C). A glassy carbon electrode with a loading mass of 0.6 mg cm^{-2} was used as working electrode. The saturated Hg/$HgCl_2$ electrode (SCE) and graphite rod were selected as the reference and counter electrodes, respectively. To prepare the working electrode, 5 mg catalyst and 1 mg acetylene black were dispersed in an aqueous solution containing 250 μL deionized water, 250 μL ethanol and 20 μL 5% Nafion solution. The obtained homogeneous catalyst ink (10 μL) was pipetted onto a polished glassy carbon electrode. The electrochemical measurement was conducted in O_2-saturated 0.1 M KOH for ORR and 1 M KOH for OER, respectively. The potential, measured against a Hg/$HgCl_2$ electrode, was converted to potential versus RHE according to E_{RHE}= 0.2415+E_{SCE}+pH*0.059. Linear sweep voltammetry (LSV) measurements were executed at a scan rate of 10 mV s^{-1}. The polarization curves of the ORR process were measured from 0 to 1.2 V (vs. RHE) in O_2-saturated solution with a sweep rate of 10 mV s^{-1} at different rotating speeds. The numbers of electrons transferred (n) during ORR was calculated by the following Koutecky-Levich equation at various electrode potentials based on the different rotating speeds:

$$\frac{1}{j}=\frac{1}{j_k}+\frac{1}{j_L}=\frac{1}{j_k}+\frac{1}{B\omega^{\frac{1}{2}}} \quad (1)$$

$$B = 0.2nFCo_2Do_2^{2/3}\upsilon^{-1/6} \quad (2)$$

where j is the measured current density, j_k and j_L are the kinetic and diffusion-limiting current densities, ω is the angular velocity, n is transferred electron number, F is the Faraday constant (96485 C mol^{-1}), C_0 is the bulk concentration of O_2 (1.2×10^{-6} mol cm^{-3} for 0.1 M KOH), D_0 is the diffusion coefficient of O_2 (1.9×10-5 cm^2 s^{-1} in 0.1 M KOH), and ν is the kinematic viscosity of the electrolyte (0.01 cm^2 s^{-1} in 0.1 M KOH). For the RRDE test, a GC disk (0.2475cm^2) surrounded by a Pt ring (0.1861cm^2) was chosen to load catalysts as working electrode. The current was collected in O_2-saturated 0.1 M KOH from GC disk and Pt ring, respectively. The electrons transferred number (n) and the hydrogen peroxide percentage ($\%H_2O_2$) during the ORR process are calculated as follows:

$$n = 4\frac{I_d}{I_d + I_r/N} \quad (3)$$

$$\%H_2O_2 = 200\frac{I_r/N}{I_r/N + I_d} \quad (4)$$

where I_d is the disk current, I_r is the ring current and N (the value is 0.37) is the collection efficiency of the Pt ring electrode.

Assembly of a zinc–air battery (ZAB)

For the Zn-air battery test, the as-prepared catalyst ink was uniformly coated onto carbon paper as the air electrode. A polished Zn plate with a thickness of 0.5 mm was used as the anode and 6 M KOH solution containing 0.2 M $Zn(AC)_2$ as the electrolyte. The mass loading was 0.62 mg cm^{-2}. For comparison, a mixture of 40% Pt/C and RuO_2 (mass ratio of 1:1) with the same loading was coated onto carbon paper

and used as the cathode. The electrochemical performances of Zn-air batteries, such as charge/discharge performance and cycling ability, were recorded by Land CT2001A system.

Supplementary figures:

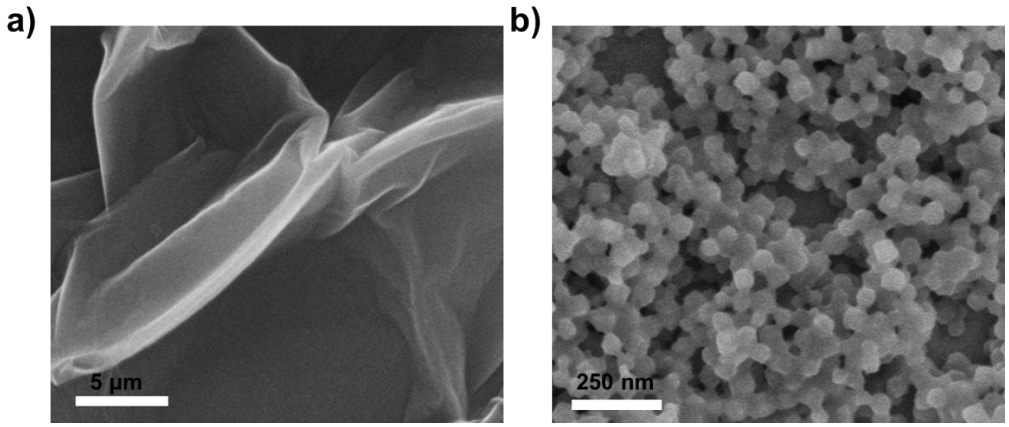

Fig. S1 SEM image of GO (a) and ZnCo-ZIF (b)

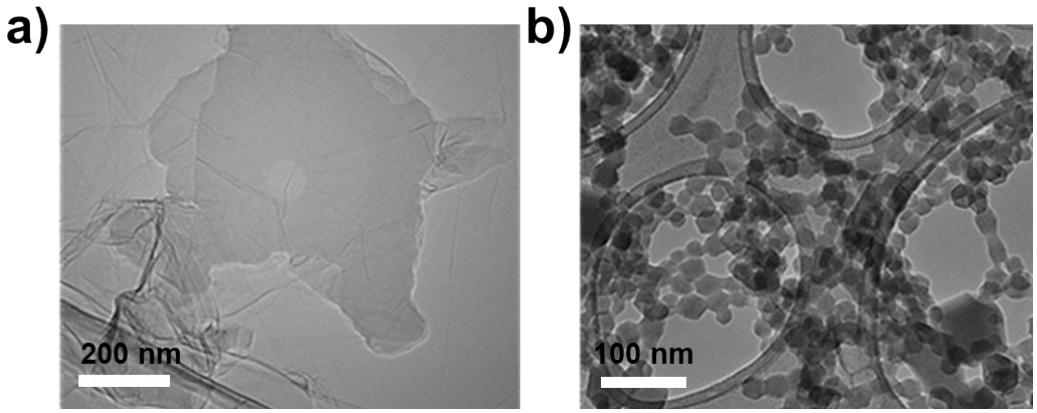

Fig. S2 TEM image of (a) GO and (b) ZnCo-ZIF

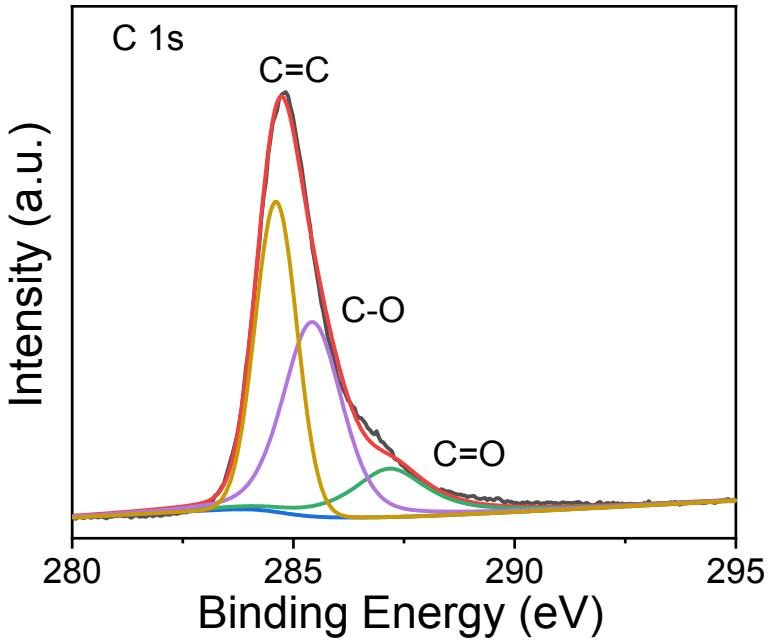

Fig. S3 High-resolution XPS spectra of C 1s fitting in ZnCo-ZIF@GO.

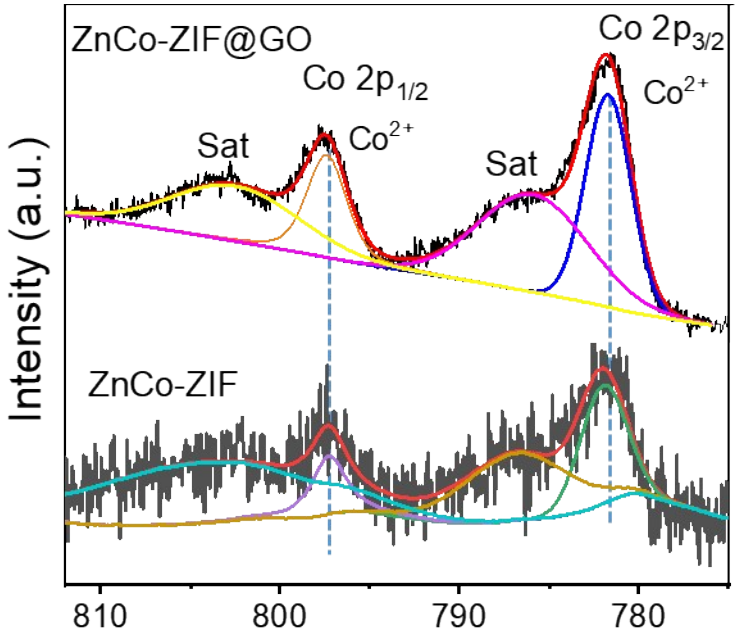

Fig. S4 High-resolution XPS spectra of Co 2p fitting in ZnCo-ZIF@GO and ZnCo-ZIF.

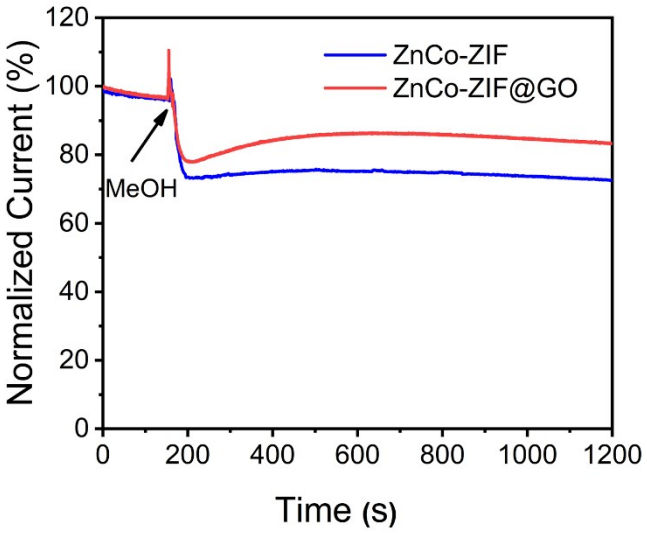

Fig. S5 Tolerance toward methanol text for ZnCo-ZIF and ZnCo-ZIF@GO

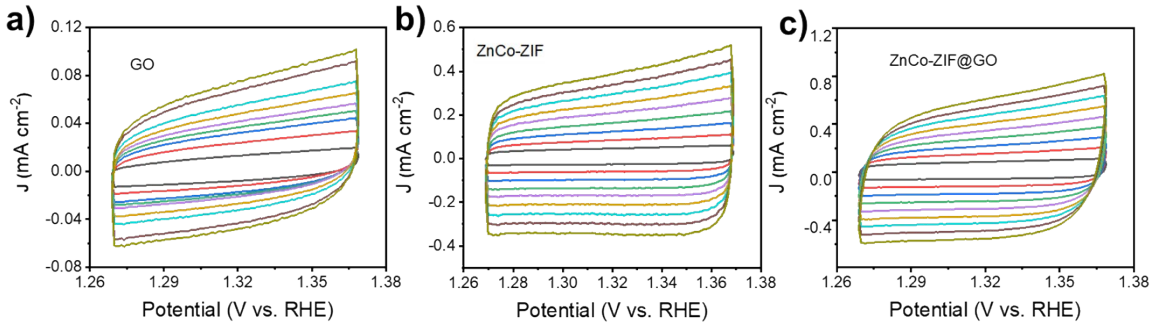

Fig. S6 cyclic voltammetry (CV) curves in the potential range of 1.27–1.37 V at different scan rates.

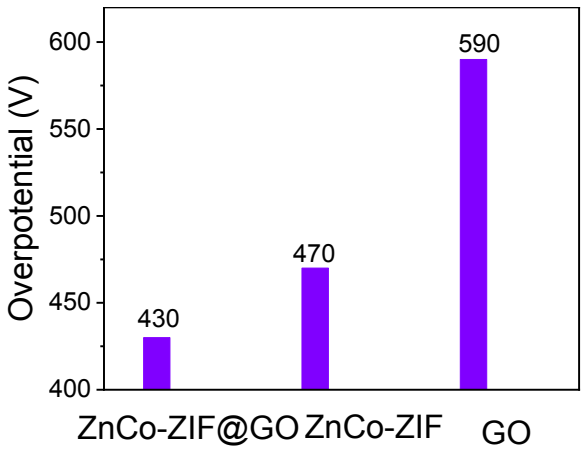

Fig. S7 Overpotential values of ZnCo-ZIF, GO and ZnCo-ZIF@GO

Supplementary Table:

Table S1 Summary on the surface areas, total pore volumes, and pore sizes of ZnCo-ZIF and ZnCo-ZIF@GO.

Sample	S_{BET} ($m^2.g^{-1}$)	V_{pore} (cm^3g^{-1})	Pore size (nm)
ZnCo-ZIF	1179	0.623	0.926
ZnCo-ZIF@GO	338.2	0.424	1.02

Table S2 Summary of recently reported catalytic performances of non-precious metal based bifunctional oxygen electrodes in 0.1 M KOH and 1 M KOH, which indicates the potential difference between ORR half-wave-potential and OER potential at 10 $mAcm^{-2}$

Catalysts	ORR onset potential (V vs. RHE)	ORR half-wave potential (V vs. RHE)	OER potential at 10 $mAcm^{-2}$ (V vs. RHE)	Refs
ZnCo-ZIF@GO	0.89	0.76	1.66	This work
ZnCo-ZIF	0.76	0.57	1.70	This work
GO	0.82	0.71	1.82	This work
$NiCo_2S_4$@N/S-rGO	0.89	0.76	1.70	[3]
$CaMnO_3$	0.89	0.76	1.77	[4]
Co_3O_4/Co_2MnO_4	0.85	0.68	1.77	[5]
LNO-NR/rGO	0.83	0.63	1.75	[6]
ε-MnO_2/MOF(Fe)	0.84	0.64	-	[7]
Co@Co_3O_4/NC-2	0.85	0..74	1.64	[8]
$NiCo_2O_4$	0.84	0.72	1.64	[9]
$LaNiO_3$/N-C	-	0.69	1.63	[10]

References

1. T. Zhou, W. Xu, N. Zhang, Z. Du, C. Zhong, W. Yan, H. Ju, W. Chu, H. Jiang, C. Wu and Y. Xie, *Adv. Mater*, 2019, **31**, e1807468.
2. J. Zhang, Z. Li, L. Zhang, J. García Molleja and D.-Y. Wang, *Carbon*, 2019, **153**, 407-416.
3. Q. Liu, J. Jin and J. Zhang *ACS Appl. Mater. Interfaces*, 2013, **5**, 5002-5008.
4. X. Han, F. Cheng, T. Zhang, J. Yang, Y. Hu and J. Chen, *Adv. Mater*, 2014, **26**, 2047-2051.
5. D. Wang, X. Chen, D. G. Evans and W. Yang, *Nanoscale*, 2013, **5**, 5312-5315.
6. J. Hu, Q. Liu, Z. Shi, L. Zhang and H. Huang, *Rsc Adv*, 2016, **6**, 86386-86394.

7. H. Wang, F. Yin, B. Chen and G. Li, *J. Mater. Chem. A,* 2015, **3**, 16168-16176.
8. A. Aijaz, J. Masa, C. Rosler, W. Xia, P. Weide, A. J. Botz, R. A. Fischer, W. Schuhmann and M. Muhler, *Angew. Chem., Int. Ed.,* 2016, **55**, 4087-4091.
9. M. Prabu, K. Ketpang and S. Shanmugam, *Nanoscale*, 2014, **6**, 3173-3181.
10. W. G. Hardin, D. A. Slanac, X. Wang, S. Dai, K. P. Johnston and K. J. Stevenson, *J. Phys. Chem. Lett*, 2013, **4**, 1254-1259.